The EMBO Journal Vol.18 No.18 pp.4926–4934, 1999

Direct nucleation and bundling of actin by the SipC protein of invasive *Salmonella*

Richard D.Hayward and Vassilis Koronakis[1]

Department of Pathology, University of Cambridge, Tennis Court Road, Cambridge CB2 1QP, UK

[1]Corresponding author
e-mail: vk103@mole.bio.cam.ac.uk

Salmonella **causes severe gastroenteritis in humans, entering non-phagocytic cells to initiate intracellular replication. Bacterial engulfment occurs by macropinocytosis, which is dependent upon nucleation of host cell actin polymerization and condensation ('bundling') of actin filaments into cables. This is stimulated by contact-induced delivery of an array of bacterial effector proteins, including the four Sips (*Salmonella* invasion proteins). Here we show *in vitro* that SipC bundles actin filaments independently of host cell components, a previously unknown pathogen activity. Bundling is directed by the SipC N-terminal domain, while additionally the C-terminal domain nucleates actin polymerization, an activity so far known only in eukaryotic proteins. The ability of SipC to cause actin condensation and cytoskeletal rearrangements was confirmed *in vivo* by microinjection into cultured cells, although as SipC associates with lipid bilayers it is possible that these activities are normally directed from the host cell membrane. The data suggest a novel mechanism by which a pathogen directly modulates the cytoskeletal architecture of mammalian target cells.**

Keywords: actin/cytoskeletal rearrangement/invasion/*Salmonella*/SipC

Introduction

Invasive bacterial pathogens promote their internalization by subverting mammalian host cell cytoskeletal dynamics (Finlay and Falkow, 1997). While the 'zipper' mechanism of *Listeria*, *Yersinia* and *Neisseria* is dictated by bacterial ligand interaction with host cell receptors, the 'trigger' mechanism of *Shigella* and *Salmonella* is driven by extensive pathogen–host cross-talk, which mimics the membrane ruffling caused by eukaryotic growth factors and culminates in bacterial uptake in a membrane-bound vacuole (Finlay and Cossart, 1997). Host cell membrane ruffling and bacterial cell entry are blocked by microfilament inhibitors like cytochalasin D (Finlay and Ruschkowski, 1991; Tran Van Nhieu and Sansonetti, 1999), indicating the essential role of actin polymerization. Actin nucleation foci are induced beneath the invading bacterium and initiate the generation of sub-membranous actin filaments (F-actin), which in turn condense into intracellular networks and cables (Finlay and Ruschkowski, 1991). As entry progresses, cellular actin-associated proteins (Adam *et al.*, 1995), microtubules (Finlay and Ruschkowski, 1991) and cell surface markers (Garcia-Del Portillo *et al.*, 1994) are recruited. The common mechanism underlying *Salmonella* and *Shigella* cell entry is dictated by the homologous *Salmonella* Sip and *Shigella* Ipa secreted effectors (Hermant *et al.*, 1995). Latex beads coated with complexes of IpaB–IpaC (SipB–SipC) proteins are internalized by HeLa cells, suggesting that these proteins are sufficient to trigger entry (Ménard *et al.*, 1996). In addition, bead uptake is associated with membrane projection, nucleation of actin polymerization and rearrangements of F-actin. Known pathogen modulators of actin function act indirectly, either by stimulating an intracellular signalling pathway involved in peripheral actin organization (Galán, 1999) or by modulating the activity of a host actin-binding protein (Tran Van Nhieu *et al.*, 1997), with the possible exception of the recently described direct interaction between *Salmonella typhimurium* SipA and F-actin (Zhou *et al.*, 1999). However, there is no example of direct pathogen-induced nucleation or bundling of actin, or indeed of a protein effecting both functions. To study the activities of *S.typhimurium* SipB and SipC, they were separately overexpressed in laboratory *Escherichia coli* and affinity purified.

Results

SipC directly bundles actin in vitro

Potential actin affinity was indicated by initial assays of co-sedimentation in which SipC sedimented in the presence of F-actin, while SipB remained entirely soluble in the supernatant (data not shown). However, even in the absence of actin, SipC solutions were extremely viscous and some SipC pelleting occurred, even when solutions were pre-clarified. Transmission electron microscopy revealed that SipC alone formed regular filamentous structures in solution (Figure 1C, middle panel) and also showed a constant light scattering trace (Figure 1B, trace C), a characteristic of soluble proteins. Gel filtration chromatography indicated a single species of ~600 kDa, suggesting that oligomerization rather than polymerization to variable lengths occurs (Figure 1A).

Light scattering and electron microscopy were used to assay the potential SipC–actin interaction *in vitro*, as co-sedimentation assays were not appropriate due to SipC oligomerization. Light scattering is positively correlated with actin filament length and is further enhanced by condensation to filament bundles (Goode *et al.*, 1999). Incubation of actin filaments with SipC stimulated large increases in F-actin light scattering (Figure 1B, trace A+C), and electron microscopy of the reaction end-points revealed a high density of F-actin bundles (Figure 1C, top panel), which could even be seen by phase-contrast light microscopy. Titration of SipC–F-actin mixtures indicated

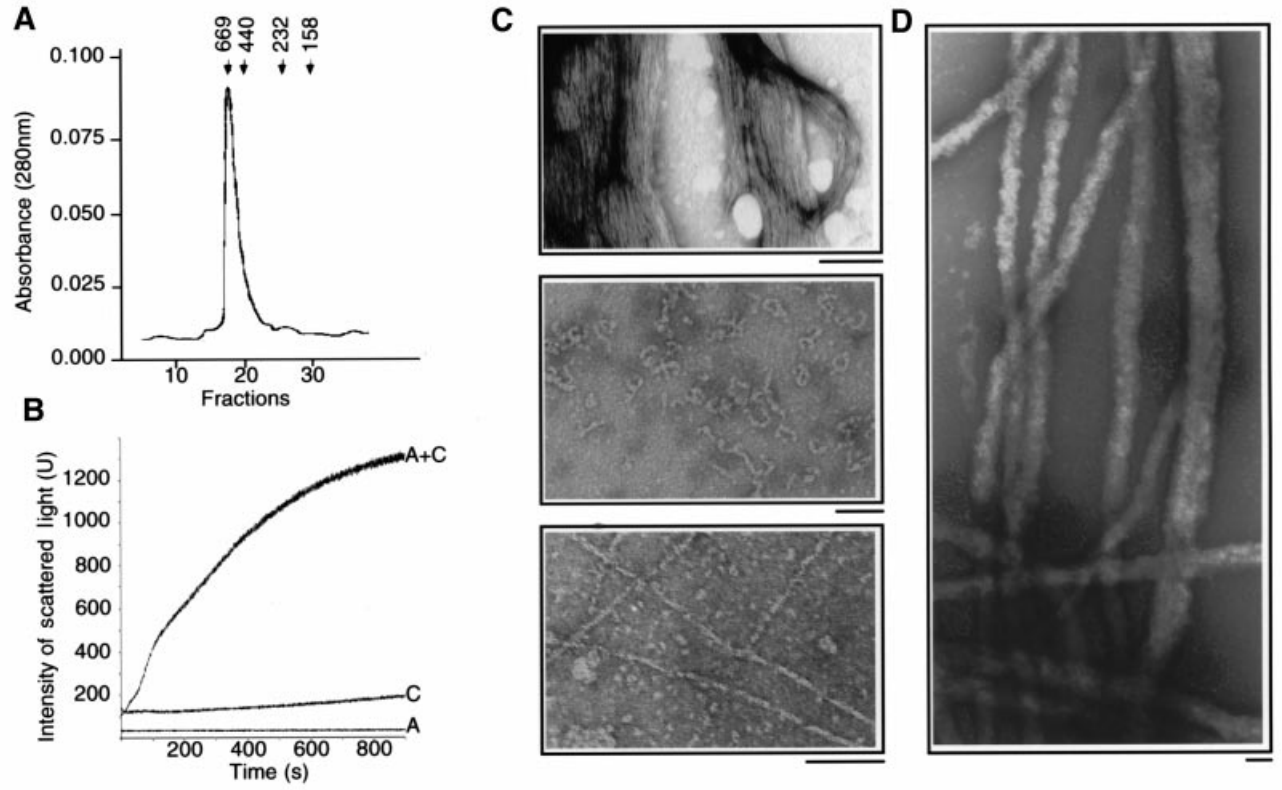

Fig. 1. Bundling of actin filaments by SipC. (**A**) SipC size estimation by chromatography. Absorbance (280 nm) of FPLC fractions of purified, refolded SipC eluting from a calibrated Superdex 200 HR10/30 column. Arrows indicate peak fractions of eluting size markers (aldolase, 158 kDa; catalase, 232 kDa; ferritin, 440 kDa; thyroglobulin, 669 kDa). (**B**) Light scattering (U, intensity at 520 nm) over 900 s by SipC alone (denoted C), F-actin alone (denoted A) and a mixture of F-actin + SipC (A+C), each component at 5 μM in F-buffer. (**C**) Transmission electron micrographs of the end-point (900 s) corresponding to light scattering traces from (B): F-actin + SipC mixture (A+C, top panel), SipC alone (C, middle panel) and F-actin alone (A, bottom panel). (**D**) Formation of actin cables from G-actin + SipC (both 5 μM) mixed after initiation of actin polymerization and sampled after 900 s incubation. All scale bars, 100 nm.

that optimal bundling occurred at a 1:1 molar ratio (data not shown). Addition of SipC to monomeric actin (G-actin) during polymerization led to comparable condensation of large F-actin cables (Figure 1D).

Distinct SipC domains effect nucleation and bundling

We sought to identify the SipC domain directing F-actin bundling, and to establish whether actin bundling might be concomitant with filament nucleation (Ménard *et al.*, 1996). The 409 amino acid SipC protein contains a predicted 80 amino acid central hydrophobic region that separates the 120 and 209 amino acid N- and C-terminal domains, respectively (Figure 2A). Both domains contain predicted coiled-coils, and the N-terminus has a proline-rich region proximal to the hydrophobic domain. Two corresponding polypeptides, SipC-N (amino acids 1–120) and SipC-C (200–409) were overexpressed in laboratory *E.coli* and purified, both remaining soluble at high concentrations. Gel filtration chromatography indicated SipC-N (15 kDa) and SipC-C (25 kDa) to be exclusively monomeric and trimeric, respectively (Figure 2B). Their effect on actin polymerization kinetics was measured *in vitro* employing pyrene-actin, a fluorescent actin derivative that has much higher fluorescence intensity as F-actin than as G-actin, although intensity values remain unaffected by subsequent F-actin bundling (Welch *et al.*, 1998). Actin alone exhibited typical assembly kinetics (Figure 2C, trace A): an initial lag-phase reflecting the kinetic barrier to 'nucleation' (the formation of G-actin trimers or tetramers), followed by rapid filament elongation, reaching steady state after 30 min. The two SipC domains had strong and strikingly distinct actin-modulating activities.

The N-terminal domain (SipC-N) did not affect actin assembly kinetics (Figure 2C, compare traces A and A+C-N). However, electron microscopy of the same sample revealed extensive F-actin pairing (Figure 2D, bottom panel), which progressed to bundling when the SipC-N peptide was present in excess (data not shown). Promotion of SipC-N induced actin bundling was confirmed by co-sedimentation. Addition of SipC-N during actin polymerization or to pre-assembled F-actin generated SipC-N–F-actin bundle complexes (Figure 3). Kinetic studies suggested that pH-independent bundling occurs within 1 min of SipC-N addition (data not shown). In contrast to the SipC N-terminal domain, the C-terminal domain (SipC-C) accelerated the kinetics of actin polymerization in the pyrene-actin assay, and the initial lag-phase was eliminated (Figure 2C, compare traces A and A+C-C). Electron microscopy revealed extended arrays of unpaired parallel actin filaments, indicating that this was due to the ability to facilitate actin filament nucleation rather than a capacity to sever newly formed filaments (Figure 2D, top panel). SipC-C clearly nucleated actin polymerization at a 1:10 (protein:actin) ratio, and the lag-phase of polymerization was eliminated at nanomolar

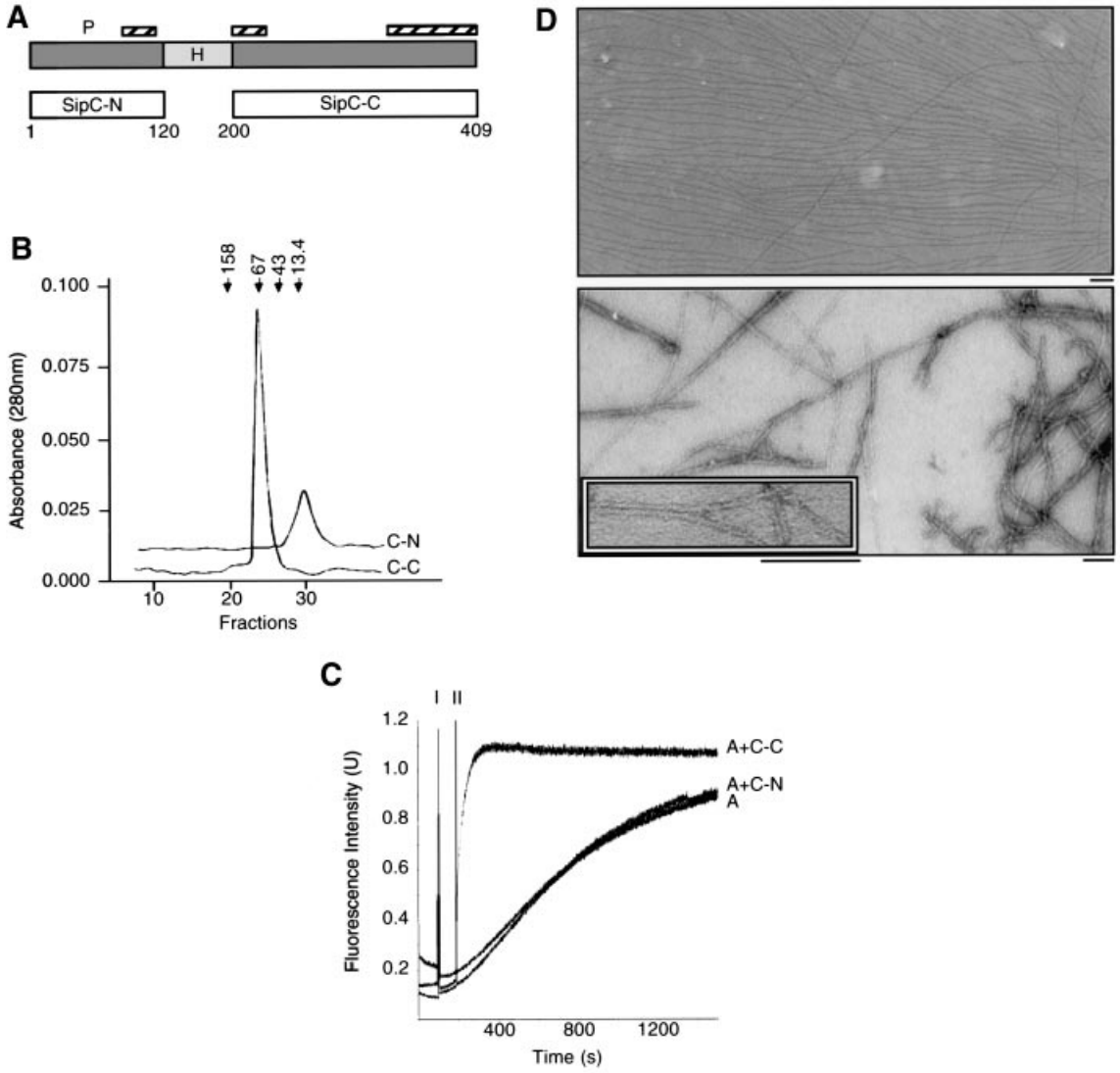

Fig. 2. Distinct actin-nucleating and actin-bundling activities of SipC. (**A**) Representation of the 409 amino acid SipC protein, showing the central 80 amino acid hydrophobic domain (H), the position of predicted coiled-coil regions (hatched bars), proline-rich sequence (P) and the 120 and 200 amino acid N-terminal (SipC-N) and C-terminal (SipC-C) peptides. Numbering indicates amino acid residues. (**B**) SipC-N and SipC-C size estimation by chromatography. Absorbance (280 nm) of FPLC fractions of purified SipC-N and SipC-C as indicated, eluting from a calibrated Superose 12 HR10/30 column. Arrows indicate peak fractions of eluting size markers (ribonuclease A, 13.4 kDa; ovalbumin, 43 kDa; BSA, 67 kDa; aldolase, 158 kDa). (**C**) Pyrene-actin assay demonstrating effects of the SipC N- and C-terminal domains on the kinetics of actin polymerization. Fluorescence intensity (excitation 365 nm, emission 395 nm) is shown over incubation time, with spike I indicating addition of initiation buffer, and spike II the addition of test peptides from 600 μM stock in 20 mM Tris–HCl pH 8. Traces show incubation of actin alone (denoted A), actin + SipC-N (A+C-N), and actin + SipC-C (A+C-C), each component at 5 μM. No fluorescence increase was observed when SipC-N or SipC-C were incubated with pyrene-labelled G-actin in G-buffer. (**D**) Transmission electron micrographs sampled at 900 s of pyrene-actin assay traces from (C). The actin + SipC-C mixture (A+C-C, top panel) shows increased numbers of single nucleated filaments, and the actin + SipC-N mixture (A+C-N, bottom panel and inset at higher magnification) shows actin filament pairing. Control actin, sampled identically, was unpaired and randomly oriented as shown in Figure 1C, lower panel. All scale bars, 100 nm.

concentrations, suggesting an activity range similar to those reported for eukaryotic nucleating proteins (for 5 μM actin: 500 nM > minimum [SipC] > 50 nM, compared with 150 nM > minimum [Arp2/3] > 37 nM; Mullins *et al.*, 1998; Welch *et al.*, 1998; Machesky *et al.*, 1999) (Figure 4A). We investigated whether SipC-C nucleated polymerization at barbed (fast-growing) rather than pointed (slow-growing) ends, since during *Shigella* invasion, actin filaments nucleate with their barbed ends facing the membrane (Adam *et al.*, 1995). Pyrene-actin assays were performed in the presence of cytochalasin D (cD), which preferentially inhibits barbed-end assembly (Cooper, 1987; Sampath and Pollard, 1991; Lanier and Volkman, 1998). When cD was included in pyrene-actin assays with SipC-C the kinetics were identical to control cD–actin (Figure 4B), indicating that filaments nucleated by SipC-C elongate predominantly from the barbed ends. When the SipC N- and C-terminal domains were mixed in an equimolar ratio, both nucleation and bundling of F-actin were achieved (Figure 4C).

SipC disrupts host cell cytoskeletal architecture in vivo

To confirm that SipC can elicit host cell cytoskeletal rearrangements *in vivo*, purified SipC was microinjected into cultured HeLa cells. Co-staining with anti-SipC poly-

clonal antibody and Texas Red-conjugated phalloidin, which has a high affinity for F-actin, permitted simultaneous visualization of intracellular SipC and the actin cytoskeleton. Thirty minutes after SipC microinjection (3 μM), injected cells exhibited dramatically increased F-actin staining and distinct zones of actin condensation (Figure 5, upper panels). Microinjection of SipC-C (3 μM or 0.3 μM) also induced a considerable increase in intracellular levels of F-actin although 'rounding-up', a cellular phenotype consistent with gross morphological change, was also evident (Figure 5, lower panels). Although SipC-N was not subject to degradation in HeLa cell extract, it could not be detected using immunostaining or on immunoprecipitation from extract (data not shown), suggesting that the polyclonal antibody did not recognize this domain in native conformation. An alternative method was therefore adopted to assay domain activity utilizing a glutathione *S*-transferase green fluorescent protein fusion (GST–GFP) as a co-injected marker. Cells were microinjected with either SipC-N or SipC-C (both 3 μM) mixed with GST–GFP or with GST–GFP alone. While both F-actin and cellular morphology remained normal in control cells injected with GST–GFP alone (Figure 6, upper panels), cytoskeletal changes were evident in cells co-injected with SipC-N (Figure 6, lower panels) or SipC-C (data not shown), indicating that both peptides were indeed active *in vivo*. Following a 20 min incubation, only 20% of cells co-injected with SipC-C remained adherent, compared with 90% of cells co-injected with SipC-N.

The microinjection procedure demonstrated that SipC

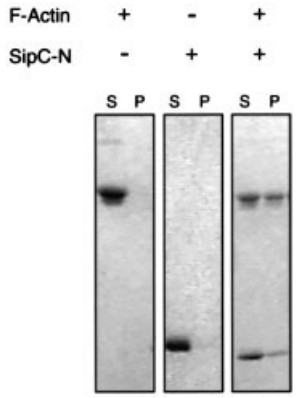

Fig. 3. Co-sedimentation of SipC N-terminus with actin bundles. Sedimentation of actin bundles from a mixture of SipC-N and F-actin (both 5 μM), demonstrating formation of an actin–SipC-N complex. Supernatants (S) and pellets (P) after centrifugation (50 000 *g*, 60 s) analysed by Coomassie Blue-stained SDS–PAGE.

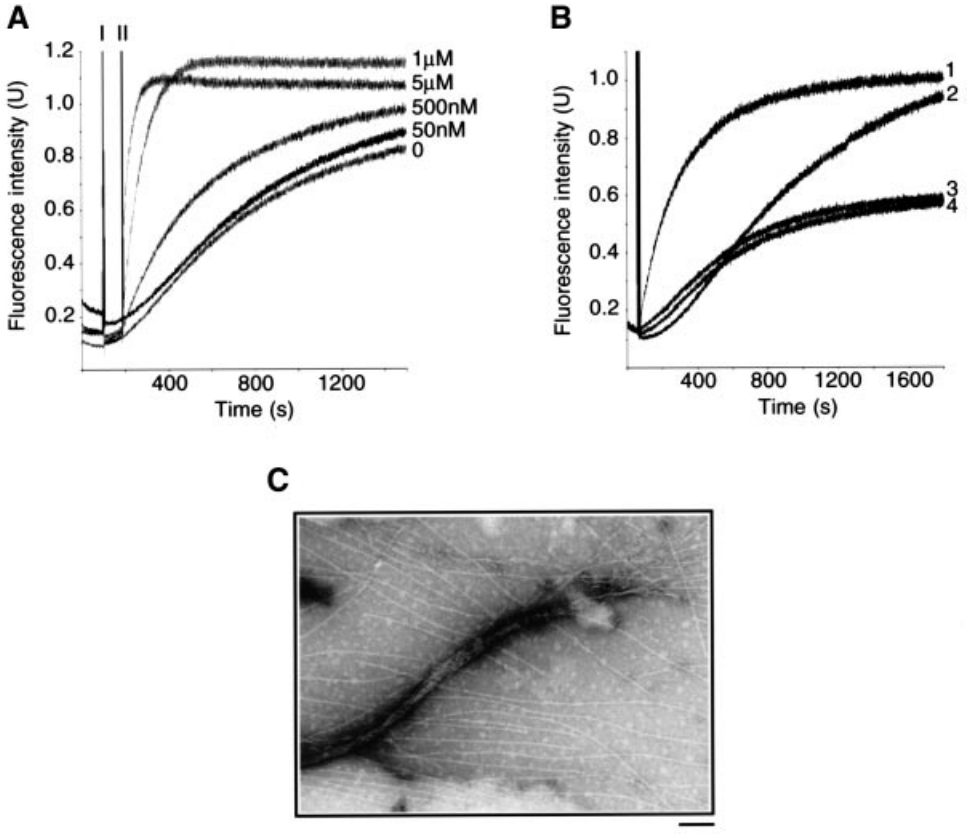

Fig. 4. SipC-C nucleates actin polymerization from barbed ends and enhances SipC-N induced actin bundling. (**A**) Pyrene-actin assay demonstrating the actin nucleation activity of the SipC C-terminal domain. Fluorescence intensity (excitation 365 nm, emission 395 nm) is shown over incubation time, with spike I indicating addition of initiation buffer, and spike II the addition of test peptide from 600 μM stock in 20 mM Tris–HCl pH 8. Traces show the effect of the addition of 5 μM, 1 μM, 500 nM, 50 nM or 0 SipC-C to 5 μM actin following initiation of polymerization. (**B**) Inhibition of actin nucleation by the SipC C-terminal domain by cD. Fluorescence intensity [as (A)] versus time for pyrene-actin assay showing actin + SipC-C (1), actin (control, 2), actin + SipC-C + cD (3) and actin + cD (4). Actin and SipC-C were at 5 μM, cD at 1 μM. cD was pre-mixed with actin prior to polymerization initiation. Spike indicates peptide addition. (**C**) Reconstitution of SipC nucleation and bundling activities. Transmission electron micrograph sampled 1800 s after mixing SipC-C + SipC-N during polymerization of actin (all 5 μM). Peptides were pre-mixed. Scale bar, 100 nm.

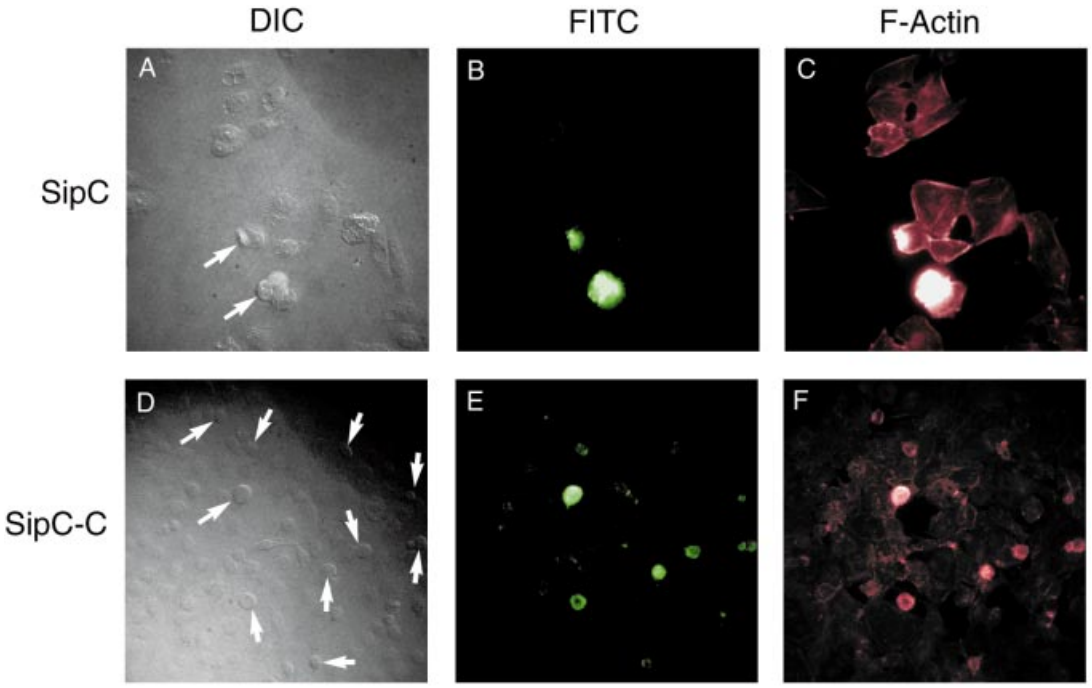

Fig. 5. Induction of cytoskeletal rearrangements *in vivo* by SipC and SipC-C microinjection. Cultured HeLa cells fixed 30 min after microinjection with purified SipC (upper panels) or SipC-C (lower panels) (3 μM). Cells (DIC; **A** and **D**) were stained with polyclonal antibody to SipC and FITC-conjugated anti-rabbit IgG [SipC (**B**), SipC-C (**E**)] and with Texas Red-conjugated phalloidin to visualize F-actin [SipC (**C**), SipC-C (**F**)]. Injected cells are indicated by arrows.

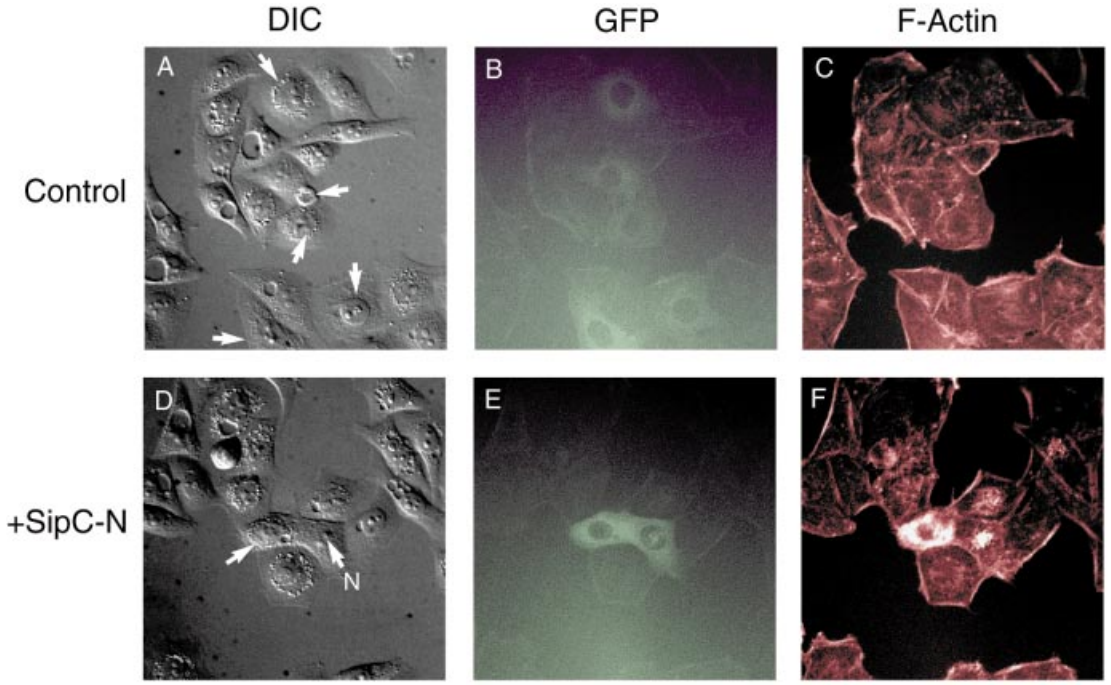

Fig. 6. Co-injection of SipC-N with GST–GFP. Cultured HeLa cells (DIC; **A** and **D**) fixed 20 min after microinjection with GST–GFP alone (upper panels) or mixed with SipC-N (lower panels) (3 μM). GST–GFP was visualized directly [GST–GFP alone (**B**); + SipC-N (**E**)] and F-actin stained with Texas Red-conjugated phalloidin [GST–GFP alone (**C**); + SipC-N (**F**)]. Injected cells are indicated by arrows (N = nuclear injection).

can disrupt actin architecture when introduced into the cytosol of mammalian cells, but does not necessarily imply that this reflects the natural location of SipC, especially as it contains a hydrophobic domain, and its *Shigella* homologue IpaC has been shown to interact *in vitro* with lipid vesicles (De Geyter *et al.*, 1997). We therefore assessed whether SipC, once delivered, might exert its action from the host cell membrane. Secreted SipC, which, as expected from study of the homologous *Shigella* IpaB–IpaC proteins (Ménard *et al.*, 1994), formed an extracellular complex with SipB (Figure 7A), did indeed associate with multilamellar lipid vesicles that mimic the composition of prokaryotic or eukaryotic membranes. The same vesicle association was also observed

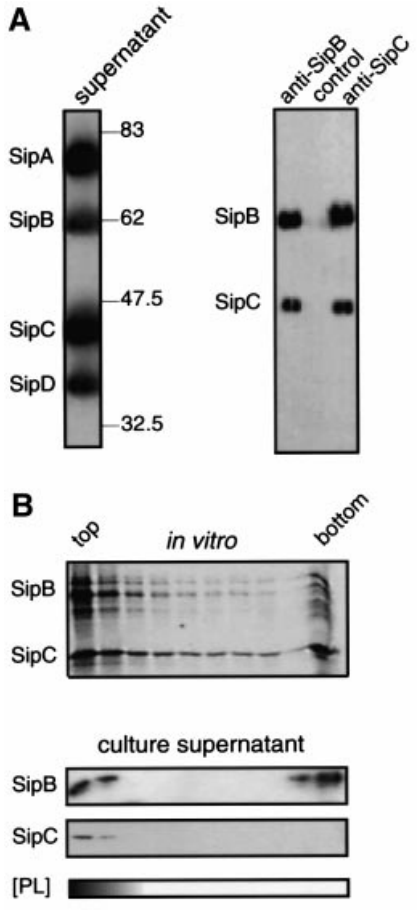

Fig. 7. Membrane association by SipC. (**A**) Immunoprecipitation of SipC–SipB complexes from *S.typhimurium* culture supernatant. Left panel: PAGE-separated *S.typhimurium* SJW1103 late-exponential culture supernatant, decorated with polyclonal antibodies raised against each of the four Sips (SipA, SipB, SipC, SipD), with positions of molecular size markers indicated in kDa. Right panel: immunoblot with polyclonal antibodies against the four Sip proteins of PAGE-separated proteins eluted from Dynabeads coupled to SipB (anti-SipB), SipC (anti-SipC) or combined pre-bleed (control) antisera. (**B**) Membrane association of SipC–SipB complexes. *In vitro* synthesized [^{35}S]Sip proteins were mixed with *E.coli* phospholipid vesicles and centrifuged through sucrose density gradients. Flotation fractions were analysed by PAGE and autoradiography (upper panel). In parallel, *S.typhimurium* SJW1103 culture supernatant was treated identically except that fractions were probed with anti-SipB or anti-SipC polyclonal antisera (lower panel). Top and bottom fractions are indicated. Phospholipid vesicles (PL), encapsulating fluorescent dye/quencher (ANTS/DPX, Molecular Probes), were tracked in identical control gradients at A_{355}, shown by shading. Comparable results were obtained with PC:PE:cholesterol multilamellar lipid vesicles.

when SipC and SipB were synthesized either alone or together in an *in vitro* transcription–translation system (Figure 7B), in contrast to a lack of association by identically synthesized SipA, SipD, SipC-N or SipC-C.

Discussion

In eukaryotic cells, actin organization is regulated by actin-associated factors, which modulate the nucleation, assembly, stabilization, cross-linking (bundling) and severing/depolymerization of actin filaments (Ayscough, 1998). Bacterial pathogens exploit such factors to allow intracellular bacterial locomotion following their internalization and cytosolic release. *Listeria* ActA (Welch *et al.*, 1997) and *Shigella* IcsA (Goldberg and Theriot, 1995) surface proteins sequester multiple cellular components such as the actin nucleation Arp2/3 complex and vasodilator-stimulated phosphoprotein (VASP), to indirectly nucleate and rearrange actin into 'comet tails' to facilitate intracellular spread (Dramsi and Cossart, 1998). Our *in vitro* experiments with purified protein indicate that SipC acts directly on actin. Separate domains nucleate polymerization and induce filament bundling in the absence of host factors, both unique activities among known bacterial virulence proteins. Interestingly, these SipC characteristics can also be interpreted in the context of the related pathogens *Shigella* and *Yersinia*. While *Yersinia* require the SipB homologue YopB for Yop effector delivery (Håkansson *et al.*, 1996), they encode no SipC homologue, as cytoskeletal rearrangements are initiated by the binding of a distinct invasin to host β_1-integrins (Tran Van Nhieu and Isberg, 1993). *Shigella* IpaC has sequence homology to the SipC actin nucleation domain, but apparently lacks the bundling domain. Our data might therefore explain how *Shigella* nucleate parallel alignments of actin filaments with their barbed ends at the membrane, but require the host actin-bundling protein T-fimbrin for efficient uptake (Adam *et al.*, 1995). This putative model assumes SipC and IpaC to be functionally homologous. In clear support of this, Tran Van Nhieu *et al.* (1999) recently presented complementary *in vivo* data consistent with IpaC being responsible for initial actin polymerization during *Shigella* entry, and indicated that actin rearrangements were dependent upon the conserved C-terminal domain. They suggested that IpaC acts indirectly, facilitating the activation of Cdc42 and Rac GTPases, but our data clearly show that SipC has the capacity to act alone. This may result only from the difference in the complementary experimental approaches, but might possibly reflect subtle variation in protein function. While the data of both Tran Van Nhieu *et al.* (1999) and ourselves demonstrate that SipC/IpaC are active in the cytosol, they do not preclude the possibility of these activities being effected from the membrane, as our control data (Figure 7) indicate.

Although the *in vivo* significance of the SipC–SipC interaction is not well defined, our observation of SipC oligomers in solution concurs with recent fluorescence anisotropy and cross-linking studies that describe homologous IpaC–IpaC, in addition to IpaB–IpaC, interactions (Davis *et al.*, 1998). The single defined gel filtration peak in Figure 1A indicates that such SipC complexes form by specific oligomerization rather than polymerization to variable lengths. Additionally, since the SipC C-terminal domain trimerizes (Figure 2B), it is tempting to speculate that this structure may contribute directly to the nucleation of G-actin trimers and also that SipC trimeric units may associate further to form higher oligomers. Once SipC–SipB complexes interact with target cell membranes, SipC or indeed SipB homo-multimerization may be a prerequisite for subsequent effector functions.

Microinjections of either purified SipC, SipC-N or SipC-C induced actin modulation *in vivo*. This occurred rapidly, within 10–30 min of microinjection, and protein activity was potent, at nanomolar final concentrations. These effects were more dramatic than those previously observed following injection of another translocated

Salmonella effector (SptP), regarded as a cytoskeletal toxin (Fu and Galán, 1998). SipC-C induced the 'rounding-up' of injected cells, indicative of either cell detachment due to uncontrolled cytoskeletal rearrangement or perhaps the induction of apoptosis. However, while a useful illustration of *in vivo* activity in support of our *in vitro* data, these results require careful interpretation. It should be emphasized that such dramatic cytoskeletal rearrangements would not occur during cell invasion, as the effect would be directed and regulated by the complex interplay between further bacterial effectors and host proteins. Additionally, it is conceivable that SipC may not be 'injected' into the cytosol. The immunofluorescence technique of Collazo and Galán (1997), which shows SipC to be distributed throughout the host cell cytoplasm, required 1–2 h of bacterium–host cell interaction before a signal could be detected. Membrane ruffling, driven by actin rearrangement, occurs much earlier during pathogen–host interplay when SipC may be associated with the host cell membrane, as our data suggest (Figure 7), but remains undetected by immunofluorescence. Purified IpaC can also interact with lipid vesicles *in vitro* (De Geyter *et al.*, 1997); membrane phospholipids may provide an additional regulatory tier, as demonstrated for the eukaryotic integral membrane actin nucleator ponticulin (Chia *et al.*, 1993). Additionally, it remains possible that cellular factors may regulate nucleation activity, for example the related eukaryotic proteins WASP and Scar, in addition to *Listeria* ActA, up-regulate the nucleation activity of Arp2/3 (Welch *et al.*, 1998; Machesky *et al.*, 1999; Rohatgi *et al.*, 1999).

A second *S.typhimurium* effector, SipA, also binds directly to actin, decreasing the critical concentration and inhibiting depolymerization of actin filaments (Zhou *et al.*, 1999). The nature of any putative interplay between SipC and SipA, which share no primary sequence homology to known eukaryotic actin-modulating proteins, remains to be determined. Invasion is dependent upon SipC (Galán, 1999) and is enhanced by SipA (Zhou *et al.*, 1999). It might be suggested that SipA could facilitate bacterial uptake by localizing and strengthening SipC-induced cytoskeletal rearrangements, or that by lowering the critical actin concentration it might influence SipC nucleation activity. Taken together with the findings of Zhou and co-workers (Zhou *et al.*, 1999), our data indicate that direct actin interaction might be a more general feature of bacterial pathogenesis than previously suspected, and suggest that actin polymerization during entry might not be determined exclusively by cellular actin nucleators downstream of Cdc42 and Rac GTPases (Chen *et al.*, 1996; Hardt *et al.*, 1998; Rohatgi *et al.*, 1999).

We suggest that following its secretion by the dedicated type III export system, SipC forms an extracellular complex with co-secreted SipB, which could be targeted to the host cell plasma membrane in proximity to the invading bacterium. SipC exposes its N- and C-termini in the host cytoplasm, allowing barbed-end actin nucleation under the membrane beneath the invading *Salmonella*, followed by filament bundling leading to condensation into actin cables (Finlay and Ruschkowski, 1991). Cytoskeletal rearrangements surrounding SipC-induced nucleation foci could be stabilized by SipA (Zhou *et al.*, 1999) and modulated by additional *Salmonella* effector proteins such as the tyrosine phosphatase SptP (Fu and Galán, 1998), the inositol phosphatase SopB (Norris *et al.*, 1998) or SopE, which interacts with Rac-1 and Cdc42 GTPases (Hardt *et al.*, 1998). These subversive proteins may indirectly recruit or down-regulate cellular actin-binding proteins and disrupt intracellular signal transduction pathways. Our data show that SipC mimics eukaryotic function, remodelling actin directly without cellular factors. Further studies of SipC will enhance understanding of eukaryotic proteins that nucleate actin, such as membrane-integral ponticulin (Chia *et al.*, 1993), exhibit bifunctional actin modulation activity (Goode *et al.*, 1999) or initiate complex processes underlying endocytosis and lamellipodial protrusion.

Materials and methods

Expression and purification of SipC recombinant proteins

Plasmid pHSipC containing the entire *sipC*, and derivatives pHSipCN (encoding amino acids 1–120) and pHSipCC (amino acids 200–409), were generated by PCR amplification from the *S.typhimurium* SJW1103 chromosome (Yamaguchi *et al.*, 1984) and cloning of PCR products, engineered to contain *Nde*I and *Bam*HI sites at the start codon ATG and 3′ of the stop codon, into the corresponding sites of T7 expression vector pET15b (Novagen), creating an N-terminal fusion of six histidine residues. Transformed *E.coli* BL21(DE3) (Studier and Moffat, 1986) cells were grown in aerated 2× tryptone yeast extract (TY) medium (50 μg/ml ampicillin, 2% glucose) at 37°C to A_{600} 1.0 and induced with 0.1 mM isopropyl-β-D-thiogalactoside (IPTG) for 2 h. Cells were pelleted (10 000 *g*, 10 min), resuspended in 1/20 culture volume and disrupted in a French Press (12 000 p.s.i., Aminco). Inclusion bodies were similarly pelleted, washed with 1 M NaCl, 2% Triton X-100 then distilled water, solubilized in binding buffer [6 M guanidine hydrochloride (GuHCl), 0.5% Triton X-100, 20 mM Tris–HCl pH 8, 150 mM NaCl, 5 mM imidazole], bound to and eluted from nickel nitrilotriacetic acid–agarose resin (Qiagen). Eluted SipC was precipitated with 80% (v/v) ethanol and repeatedly washed with water to remove detergent before resuspension and concentration in 4 M GuHCl to 600 μM. SipC-N and SipC-C were dialysed against 5× 5 l 20 mM Tris–HCl pH 7.4, loaded on to anion exchange chromatography (SipC-N) or heparin affinity (SipC-C) columns (PerSeptive Biosystems, 1.7 ml), washed with 50 column-volumes 20 mM Tris–HCl pH 7.4 and eluted using 20 mM Tris–HCl pH 7.4, 0.5 M NaCl. Following final dialysis against 5 l 20 mM Tris–HCl pH 8, both peptides were concentrated to 600 μM. Proteins were assayed with a Coomassie Blue-based staining solution (Pierce).

Gel filtration chromatography

Samples of 1.0 mg/ml purified SipC, SipC-N or SipC-C in a maximum volume of 0.2 ml were injected on to either a Superdex 200 HR10/30 or Superose 12 HR10/30 column (Pharmacia), equilibrated with 20 mM Tris–HCl pH 7.4, 120 mM NaCl and developed at 0.5 ml/min. Protein elution was monitored by absorbance at 280 nm using an in-line detector (Waters 486).

Microinjection and fluorescence microscopy

SipC (600 μM) in 4 M GuHCl was diluted to 3 μM in, and dialysed against, 1 mM 2-[*N*-Morpholino]ethanesulfonic acid (MES) pH 6. SipC-C and SipC-N stocks (600 μM) in 20 mM Tris–HCl pH 8 were diluted in 1 mM MES. Control GST–GFP was diluted in the same buffer. HeLa cells were grown to sub-confluency on poly-L-lysine-treated 13 mm round coverslips (Sarstedt) in Dulbecco's modified Eagle's medium (DMEM), supplemented with 10% (v/v) fetal calf serum, L-glutamine and penicillin/streptomycin. Purified proteins, filtered and clarified by centrifugation, were microinjected into the cytoplasm of HeLa cells using a semi-automatic microinjector and a micromanipulator (Eppendorf). Cells were fixed after injection in 3.7% formaldehyde, permeabilized in the presence of 0.2% Triton X-100 for 3 min, washed in phosphate buffered saline (PBS) containing 3% (w/v) bovine serum albumin (BSA) and sequentially incubated with 1:250 dilution SipC polyclonal antibody in PBS/BSA for 1 h at room temperature and fluorescein isothiocyanate (FITC)-conjugated anti-rabbit IgG (Vector Laboratories) diluted 1:100 in PBS/BSA and 5 μg/ml Texas Red-conjugated phalloidin for 30 min (Molecular Probes). Following GST–GFP injection experiments, cells were fixed, permeabilized and stained directly for 20 min with 5 μg/ml

Texas Red-conjugated phalloidin in PBS. Coverslips were mounted on to slides and visualized under a fluorescence microscope (Leica DM IRBE).

Immunoblots and immunoprecipitation

Aliquots (500 µl) of *S.typhimurium* SJW1103 culture supernatant from late-exponential aerobic cultures in 2× TY, were clarified by two successive centrifugations (13 000 *g*) and filtration (0.2 µm, Gelman Sciences), incubated (30 min) with M-280 sheep anti-rabbit IgG Dynabeads (Dynal, prewashed in PBS) and coupled to anti-SipB, anti-SipC or combined pre-bleed polyclonal antisera with additional 3% (w/v) BSA. Following collection by a Magnetic Particle Collector (Dynal), beads were washed three times with PBS/BSA, bound proteins eluted into Laemmli sample buffer and boiled for 3 min prior to SDS–PAGE. Samples were blotted and probed with polyclonal antisera raised in rabbits (Scottish Antibody Production Unit, Carluke, UK) immunized with affinity-purified *Salmonella* Sips overexpressed in *E.coli*.

Membrane flotation

In vitro transcription–translation reactions (50 µl) (Bailey *et al.*, 1996) included a 50 µM amino acid mixture and [^{35}S]methionine (Amersham), 2.5 µg purified T7 RNA polymerase and 250 ng supercoiled template, pARSipB and pARSipC [*sipB* or *sipC* expressed from T7 promoter in pAR3040 (Studier and Moffat, 1986), respectively]. *In vitro* reactions, or 100 µl aliquots of *S.typhimurium* SJW1103 late-exponential culture supernatants as appropriate, were mixed with either purified *E.coli* phospholipids or phosphatidylcholine:phosphatidylethanolamine:cholesterol (2:1:1) mixture (10 mM HEPES pH 7.4, 120 mM NaCl; Avanti Polar Lipids) at room temperature for 10 min. Samples were mixed directly with 55% (w/v) sucrose, overlaid with 40% (w/v) sucrose and centrifuged (16 h, 75 000 *g*, 16°C), before fractionation (10 × 500 µl) and precipitation with 10% (v/v) trichloroacetic acid.

Actin bundling and assembly

F-actin bundling was monitored either by light scattering (excitation 520 nm, emission 520 nm, slit widths 2.5 nm) in an LS50B fluorescence spectrophotometer (Perkin Elmer), or by a pelleting assay. Protein samples were added either to F-actin pre-assembled from purified rabbit skeletal muscle actin (5 µM) in G-buffer (5 mM Tris–HCl pH 8, 0.1 mM ATP, 0.2 mM $CaCl_2$, 0.02% NaN_3) by the addition of 0.02 vol 50× initiation buffer (100 mM $MgCl_2$, 50 mM ATP, 2.5 M KCl) (Cytoskeleton Inc.) and incubated for 30 min at 25°C, or during assembly where required. Comparable light scattering results were obtained using control non-His-tagged SipC, purified identically except for the final affinity column. For co-sedimentation, reactions were centrifuged at 50 000 *g* (1 min, 16°C) and the supernatants and pellets analysed by SDS–PAGE and Coomassie Blue staining. Actin filaments remain in the supernatant under these conditions, whereas F-actin bundles pellet (Goode *et al.*, 1999). Pyrene fluorescence was monitored by spectrophotometry (excitation 365 nm, emission 395 nm, slit widths 5 nm) and data analysed using FLWinLab software (Perkin Elmer). Pyrene-labelled G-actin and unlabelled G-actin were mixed 1:10 in fresh G-buffer (5 µM) and centrifuged to remove F-actin. Actin polymerization was triggered using 0.02 vol 50× initiation buffer. Purified peptides or control buffers were added before or during polymerization. His-tag alone has no effect on the polymerization of actin (Welch *et al.*, 1998).

Electron microscopy

Proteins were adsorbed on to freshly glow-discharged, carbon-coated copper grids for 1–2 min and washed in water before negative staining (Harris, 1997) with 2% uranyl acetate, 2% phosphotungstic acid (PTA) pH 7.0 or 2% ammonium molybdate pH 7.0. Grids were examined using a Philips CM100 transmission electron microscope operated at 80 kV.

Acknowledgements

We thank Emma McGhie for preparation of SipC peptides; Jeremy Skepper (Multi-Imaging Centre, University of Cambridge) for assistance with electron microscopy; Alan Weeds and Brian Pope (Medical Research Council Laboratory of Molecular Biology, Cambridge) for gifts of purified actin, pyrene-actin and discussions; Anja Hagting and Jonathon Pines (Wellcome Trust and Cancer Research Campaign Institute of Cancer and Developmental Biology, University of Cambridge) for invaluable assistance with microinjection experiments and for the gift of GST–GFP protein; and Eva Koronakis and Colin Hughes for critical discussion of this manuscript. This work was supported by a Wellcome Trust grant to V.K. and a Medical Research Council Studentship to R.D.H.

References

Adam,T., Arpin,M., Prévost,M.-C., Gounon,P. and Sansonetti,P.J. (1995) Cytoskeletal rearrangements and the functional role of T-plastin during entry of *Shigella flexneri* into HeLa cells. *J. Cell Biol.*, **29**, 367–381.

Ayscough,K.R. (1998) *In vivo* functions of actin-binding proteins. *Curr. Opin. Cell Biol.*, **10**, 102–111.

Bailey,M.J.A., Hughes,C. and Koronakis,V. (1996) Increased distal gene transcription by the elongation factor RfaH, a specialised homologue of NusG. *Mol. Microbiol.*, **22**, 729–737.

Chen,L.M., Hobbie,S. and Galán,J.E. (1996) Requirement of CDC42 for *Salmonella*-induced cytoskeletal and nuclear responses. *Science*, **274**, 2115–2118.

Chia,C.P., Shariff,A., Savage,S.A. and Luna,E.J. (1993) The integral membrane protein, ponticulin, acts as a monomer in nucleating actin assembly. *J. Cell Biol.*, **120**, 909–922.

Collazo,C.M. and Galán,J.E. (1997) The invasion-associated type III system of *Salmonella typhimurium* directs the translocation of Sip proteins into the host cell. *Mol. Microbiol.*, **24**, 747–756.

Cooper,J.A. (1987) Effects of cytochalasin and phalloidin on actin. *J. Cell Biol.*, **105**, 1473–1478.

Davis,R., Marquart,M.E., Lucius,D. and Picking,W.D. (1998) Protein–protein interactions in the assembly of *S.flexneri* invasion plasmid antigens IpaB and IpaC into protein complexes. *Biochim. Biophys. Acta*, **1429**, 45–56.

De Geyter,C., Vogt,B., Benjelloun-Touimi,Z., Sansonetti,P.J., Ruysschaert,J.-M., Parsot,C. and Cabiaux,V. (1997) Purification of IpaC, a protein involved in entry of *Shigella flexneri* into epithelial cells and characterisation of its interaction with lipid membranes. *FEBS Lett.*, **400**, 149–154

Dramsi,S. and Cossart,P. (1998) Intracellular pathogens and the actin cytoskeleton. *Annu. Rev. Cell Dev. Biol.*, **14**, 137–166.

Finlay,B.B. and Cossart,P. (1997) Exploitation of mammalian host cell functions by bacterial pathogens. *Science*, **276**, 718–725.

Finlay,B.B. and Falkow,S. (1997) Common themes in microbial pathogenicity revisited. *Microbiol. Mol. Biol. Rev.*, **61**, 136–169.

Finlay,B.B. and Ruschkowski,S. (1991) Cytoskeletal rearrangements accompanying *Salmonella* entry into epithelial cells. *J. Cell Sci.*, **99**, 283–296.

Fu,Y. and Galán,J.E. (1998) The *S.typhimurium* tyrosine phosphatase SptP is translocated into host cells and disrupts the actin cytoskeleton. *Mol. Microbiol.*, **27**, 359–368.

Galán,J.E. (1999) Interaction of *Salmonella* with host cells through the centisome 63 type III secretion system. *Curr. Opin. Microbiol.*, **2**, 46–50.

Garcia-Del Portillo,F., Pucciarelli,M.G., Jefferies,W.A. and Finlay,B.B. (1994) *Salmonella typhimurium* induces selective aggregation and internalization of host cell surface proteins during invasion of epithelial cells. *J. Cell Sci.*, **107**, 2005–2020.

Goldberg,M.A. and Theriot,J.A. (1995) *S.flexneri* surface protein IcsA is sufficient to direct actin-based motility. *Proc. Natl Acad. Sci. USA*, **92**, 6572–6576.

Goode,B.L., Wong,J.J., Butty,A.-C., Peter,M., McCormack,A.L., Yates,J.R., Drubin,D.G. and Barnes,G. (1999) Coronin promotes the rapid assembly and cross-linking of actin filaments and may link the actin and microtubule cytoskeletons in yeast. *J. Cell Biol.*, **144**, 83–98.

Håkansson,S., Schesser,K., Persson,C., Galyov,E.E., Rosqvist,R., Homblé,F. and Wolf-Watz,H. (1996) The YopB protein of *Yersinia* is essential for the translocation of Yop effector proteins across the target cell plasma membrane and displays contact dependent membrane disrupting activity. *EMBO J.*, **15**, 5812–5823.

Hardt,W.-D., Chen,L.-M, Schuebel,K.E., Bustelo,X.R. and Galán,J.E. (1998) *Salmonella typhimurium* encodes an activator of Rho GTPases that induces membrane ruffling and nuclear responses in host cells. *Cell*, **93**, 815–826.

Harris,J.R. (1997) *Negative Staining and Cryoelectron Microscopy.* βIOS Scientific Publishers, Oxford, UK, in association with the Royal Microscopical Society.

Hermant,D., Ménard,R., Arricau,N., Parsot,C. and Popoff,M.Y. (1995) Functional conservation of the *Salmonella* and *Shigella* effectors of entry into epithelial cells. *Mol. Microbiol.*, **17**, 781–789.

Lanier,L.M. and Volkman,L.E. (1998) Actin binding and nucleation by *Autographa california* M nucleopolyhedrovirus. *Virology*, **243**, 167–177.

Machesky,L.M., Mullins,R.D., Higgs,H.N., Kaiser,D.A., Blanchoin,L., May,R.C., Hall,M.E. and Pollard,T.D. (1999) Scar, a WASp-related protein, activates nucleation of actin filaments by the Arp2/3 complex. *Proc. Natl Acad. Sci. USA*, **96**, 3739–3744.

Ménard,R., Sansonetti,P., Parsot,C. and Vasselon,T. (1994) Extracellular association and cytoplasmic partitioning of the IpaB and IpaC invasins of *Shigella flexneri. Cell*, **79**, 515–525.

Ménard,R., Prévost,M.C., Gounon,P., Sansonetti,P.J. and Dehio,C. (1996) The secreted Ipa complex of *Shigella flexneri* promotes entry into mammalian cells. *Proc. Natl Acad. Sci. USA*, **93**, 1254–1258.

Mullins,R.D., Henser,J.A. and Pollard,T.D. (1998) The interaction of Arp2/3 complex with actin: nucleation, high affinity pointed end capping and formation of branching networks of filaments. *Proc. Natl Acad. Sci. USA*, **95**, 6181–6186.

Norris,F.A., Wilson,M.P., Wallis,T.S., Galyov,E.E. and Majerus,P.W. (1998) SopB, a protein required for virulence of *S.dublin*, is an inositol phosphate phosphatase. *Proc. Natl Acad. Sci. USA*, **95**, 14057–14059.

Rohatgi,R., Ma,L., Miki,H., Lopez,M., Kirchhausen,T., Takenawa,T. and Kirschner,M.W. (1999) The interaction between N-WASP and the Arp2/3 complex links Cdc42-dependent signals to actin assembly. *Cell*, **97**, 221–231.

Sampath,P. and Pollard,T.D. (1991) Effects of cytochalasin, phalloidin and pH on the elongation of actin filaments. *Biochemistry*, **30**, 1973–1980.

Studier,W. and Moffat,B.A. (1986) Use of bacteriophage T7 RNA polymerase to direct selective high level expression of cloned genes. *J. Mol. Biol.*, **189**, 113–130.

Tran Van Nhieu,G. and Isberg,R.R. (1993) Bacterial internalization mediated by β_1 chain integrins is determined by ligand affinity and receptor density. *EMBO J.*, **12**, 1887–1895.

Tran Van Nhieu,G. and Sansonetti,P.J. (1999) Mechanism of *Shigella* entry into epithelial cells. *Curr. Opin. Microbiol.*, **2**, 51–55.

Tran Van Nhieu G., Ben Ze'ev,A. and Sansonetti,P.J. (1997) Modulation of bacterial entry into epithelial cells by interaction between vinculin and *Shigella* IpaA invasin. *EMBO J.*, **16**, 2717–2729.

Tran Van Nhieu,G., Caron,E., Hall,A. and Sansonetti,P.J. (1999) IpaC induces actin polymerization and filopodia formation during *Shigella* entry into epithelial cells. *EMBO J.*, **18**, 3249–3262.

Welch,M.D., Iwamatsu,A. and Mitchison,T.J. (1997) Actin polymerisation is induced by Arp2/3 protein complex at the surface of *Listeria. Nature*, **385**, 265–269.

Welch,M.D., Rosenblatt,J., Skoble,J., Portnoy,D.A. and Mitchison,T.J. (1998) Interaction of human Arp2/3 complex and the *Listeria monocytogenes* ActA protein in actin filament nucleation. *Science*, **281**, 105–108.

Yamaguchi,S., Fujita,H., Sugata,K., Taira,T. and Iino,T. (1984) Genetic analysis of H2, the structural gene for phase-2 flagellin in *Salmonella*. *J. Gen. Microbiol.*, **130**, 255–265.

Zhou,D., Mooseker,M.S. and Galán,J.E. (1999) Role of the *S.typhimurium* actin-binding protein SipA in bacterial internalisation. *Science*, **283**, 2092–2095.

Received June 3, 1999; revised and accepted July 21, 1999